NeuroImage 62 (2012) 2021–2033

Contents lists available at SciVerse ScienceDirect

NeuroImage

journal homepage: www.elsevier.com/locate/ynimg

Classifying minimally disabled multiple sclerosis patients from resting state functional connectivity

Jonas Richiardi [a,b,*], Markus Gschwind [c,d,e], Samanta Simioni [c], Jean-Marie Annoni [d,e,f], Beatrice Greco [g], Patric Hagmann [h,i], Myriam Schluep [c], Patrik Vuilleumier [d,e], Dimitri Van De Ville [a,b]

[a] Department of Radiology and Medical Informatics, University of Geneva, Geneva, Switzerland
[b] Institute of Bioengineering, Ecole Polytechnique Fédérale de Lausanne (EPFL), Lausanne, Switzerland
[c] Department of Clinical Neurosciences, Centre Hospitalier Universitaire Vaudois (CHUV) and University of Lausanne, Lausanne, Switzerland
[d] Department of Neurology, Hopitaux Universitaires de Genève (HUG), Geneva, Switzerland
[e] Department of Neuroscience, University Medical Center (CMU), University of Geneva, Geneva, Switzerland
[f] Neurology unit, University of Fribourg, Fribourg, Switzerland
[g] Merck-Serono, Geneva, Switzerland
[h] Department of Medical Radiology, Centre Hospitalier Universitaire Vaudois (CHUV) and University of Lausanne, Lausanne, Switzerland
[i] Signal Processing Lab 5, Ecole Polytechnique Fédérale de Lausanne (EPFL), Lausanne, Switzerland

ARTICLE INFO

Article history:
Accepted 28 May 2012
Available online 5 June 2012

Keywords:
Brain decoding
Brain networks
Classification
Functional magnetic resonance imaging
Imaging marker

ABSTRACT

Multiple sclerosis (MS), a variable and diffuse disease affecting white and gray matter, is known to cause functional connectivity anomalies in patients. However, related studies published to-date are post hoc; our hypothesis was that such alterations could discriminate between patients and healthy controls in a predictive setting, laying the groundwork for imaging-based prognosis. Using functional magnetic resonance imaging resting state data of 22 minimally disabled MS patients and 14 controls, we developed a predictive model of connectivity alterations in MS: a whole-brain connectivity matrix was built for each subject from the slow oscillations (<0.11 Hz) of region-averaged time series, and a pattern recognition technique was used to learn a discriminant function indicating which particular functional connections are most affected by disease. Classification performance using strict cross-validation yielded a sensitivity of 82% (above chance at $p<0.005$) and specificity of 86% ($p<0.01$) to distinguish between MS patients and controls. The most discriminative connectivity changes were found in subcortical and temporal regions, and contralateral connections were more discriminative than ipsilateral connections. The pattern of decreased discriminative connections can be summarized post hoc in an index that correlates positively ($\rho=0.61$) with white matter lesion load, possibly indicating functional reorganisation to cope with increasing lesion load. These results are consistent with a subtle but widespread impact of lesions in white matter and in gray matter structures serving as high-level integrative hubs. These findings suggest that predictive models of resting state fMRI can reveal specific anomalies due to MS with high sensitivity and specificity, potentially leading to new non-invasive markers.

Introduction

Multiple sclerosis (MS) is a common neurological disease, especially among the young in northern countries and is characterized by recurrent or progressive inflammatory events that lead to spatially disseminated demyelination of the central nervous system, followed by subsequent axonal loss (Compston and Coles, 2008). Early treatment is important to avoid permanent damage and might slow or delay progression (Jacobs et al., 2000; Kappos et al., 2007). However, due to the variety of clinical presentations and its large differential diagnosis, early identification of the disease is especially problematic (Rolak and Fleming, 2007; Swanton et al., 2007). In its most common relapsing–remitting form (RRMS), patients present attacks alternating with episodes of clinical improvements, following an unpredictable rhythm (Noseworthy et al., 2000). Current diagnostic workup is based on clinical examination together with structural magnetic resonance imaging (MRI) of brain and spine as well as cerebrospinal fluid analysis, seeking for evidence of both dissemination in time and dissemination in space of the inflammatory lesions (Compston and Coles, 2008). The role of MRI, most often relying on T2-weighted and gadolinium-enhanced images to establish the diagnosis, is of growing importance to establish the diagnosis and follow disease progression or remission (Barkhof et al., 2009; Polman et al., 2005, 2011). However, conventional MRI has several recognized limitations; the "hidden" damage known to occur in the normal appearing brain tissue (NABT) (Fu et al., 1998) is not captured; structural lesions are not always specific to MS (Barkhof and Filippi, 2009; multiple sclerosis MRI surrogate); T2 hyperintensities are histologically unspecified since inflammation and demyelination as

* Corresponding author at: EPFL/IBI-STI/GRVDV, Station 17, 1015 Lausanne, Switzerland.
E-mail address: jonas.richiardi@epfl.ch (J. Richiardi).

1053-8119/$ – see front matter © 2012 Elsevier Inc. All rights reserved.
doi:10.1016/j.neuroimage.2012.05.078

well as axonal damage and gliosis have similar signal characteristics (Ratchford and Calabresi, 2008); and the correlation of lesion load and clinically significant impairment is poor (Barkhof, 2002; Filippi and Agosta, 2010). Therefore, current radiological signs obtained from structural MRI may not reflect the actual disease state.

In this context, interest is growing for alternative MRI modalities that may provide complementary information, with the aim of finding additional imaging markers for MS (Filippi and Agosta, 2010). One such modality is diffusion MRI: there is evidence that axial diffusion is relatively specific to axonal degeneration (Song et al., 2003), while increased radial diffusion is mainly driven by demyelination (Budde et al., 2009; Zhu et al., 1999. The use of advanced tractography methods suggests that a connectional framework may lead to improved sensitivity and specificity to the disease and its related clinical impairment (Ciccarelli et al., 2005; Lin et al., 2005; Dineen et al., 2009).

Another technique that also builds on the connectional framework and has potential sensitivity to detect "invisible" lesions is functional MRI (fMRI). Based on the blood oxygen level dependent (BOLD) signal, this technique gives an indirect measure of aggregate neuronal excitation-inhibition in gray matter microcircuits (Logothetis, 2008). MS lesions can alter neuronal networks in several ways. Several fMRI studies have highlighted brain circuit plasticity and its potentially adaptive role in recovery or compensation in response to brain lesions (Reddy et al., 2000b), for motor (e.g., finger tapping) (Lee et al., 2000; Morgen et al., 2004; Reddy et al., 2000a) as well as cognitive tasks (e.g., working memory and attention tasks) (Mainero et al., 2004; Morgen et al., 2007). While permanent axonal changes already accompany even early acute inflammatory responses (Trapp et al., 1998), fMRI studies indicate that adaptive plasticity might limit the initial clinical expression of the disease (Cifelli and Matthews, 2002; Rocca and Filippi, 2007) and that patients can show complete clinical recoveries after relapses, explaining the missing link between clinical and radiological presentation. Pathological functional effects have been shown, as for example the loss of interhemispheric inhibition, related to corpus callosum atrophy (Manson et al., 2006, 2008). A negative effect of disease progression on plasticity has also become clear, limiting the potential for adaptive capacity and leading to globally reduced brain connectivity and dysfunction (Cader et al., 2006; Morgen et al., 2004).

Furthermore, beyond local changes in activity, fMRI can provide information on the architecture and interconnectivity of more distributed brain networks, notably by measuring patterns of spontaneous fluctuations during resting state (Biswal et al., 1995; Greicius et al., 2003). Resting state connectivity analysis has benefitted from recent advances in fMRI methodology allowing to investigate intrinsic (i.e., not task related) brain activity across the whole brain and to identify the degree of functional correlation between distant areas (Greicius et al., 2009). Many publications have focused on analyzing the default mode network (DMN) (Buckner et al., 2008), a set of regions highly synchronized during rest. This methodology has been used in several diseases characterized by diffuse lesions (Fox and Greicius, 2010) such as schizophrenia (Jafri et al., 2008), Alzheimer's disease (Greicius et al., 2004; Li et al., 2002) or depression (Greicius et al., 2007), but investigations in MS are limited to relatively fewer publications. For example, Cover et al. (2006) found decreased inter-hemispheric connectivity in MS patients at rest, using a coherence measure based on magnetoencephalography (MEG). Rocca et al. (2010) found reduction of activity in the anterior cingulate cortex (ACC) at rest in MS patients relative to controls and in cognitively impaired MS patients related to cognitively intact MS patients. Weaker DMN connectivity in the ACC of MS patients was also reported by Bonavita et al. (2011) using independent component analysis of fMRI resting state data. Roosendaal et al. (2010) investigated fMRI resting state networks in patients with clinically isolated syndrome (CIS) and patients with RRMS and observed an increased synchronization of some resting state networks in CIS patients, which disappeared in those with RRMS, suggesting initial functional compensation that is lost with disease progression. Using ICA and seed correlation, Jones et al. (2011) showed significant differences in connectivity at rest between a single MS patient with an important thalamic lesion and a group of controls, in particular, in the default mode network.

Based on these studies, resting state fMRI offers a promising avenue to further investigate the functional impact of pathology, including at early stages of MS where long-range connectivity can be altered by both inflammatory processes and mild axonal damage. However, a comprehensive assessment of altered brain connectivity would need to detect subtle and distributed patterns throughout the brain, in a data-driven and objective manner despite the highly variable location of lesions in MS. Moreover, for both task-based activity and resting state connectivity analyses, functional changes and compensatory mechanisms can appear either as increases or decreases, depending on the task, individual patient, and/or disease state. Given the high number of possible connections to test, mass-univariate or summary statistics have difficulties to find significant differences; e.g., mean connectivity between specific regions of interest may show no consistent differences between MS and controls (Lowe et al., 2008). Instead, here we propose the use of *predictive* multivariate models that can generalize to unseen subjects (those not used to learn the parameters of a model) and thus potentially lead to a new imaging-based marker for MS. Recent work has highlighted the feasibility of using single structural scans for reliable MS diagnosis (Rovira et al., 2009), the ability of local multivariate predictive methods to discriminate between MS patients and controls with high accuracy, even when using NABT structural data (Weygandt et al., 2011), and the possibility of using global multivariate methods with structural data to distinguish various aspects of MS severity (Bendfeldt et al., 2012). Accordingly, given the increased use and development of predictive modeling techniques in fMRI research, originally derived from machine learning or pattern recognition (Ethofer et al., 2009; Kamitani and Tong, 2005; Mourao-Miranda et al., 2005; Shirer et al., 2011; Weil and Rees, 2010), it would appear highly suitable and advantageous to apply similar techniques to characterize high-dimensional fMRI data obtained during resting state (Richiardi et al., 2010, 2011). There has also been a slow concurrent increase in the use of multivariate predictive modeling techniques applied to functional connectivity data of pathological subjects. For example, Craddock et al. (2009) have proposed using the temporal pairwise correlations between 15 expertly selected regions of interest as features for a support vector machine classifier applied to depressive patients. More recently, Chen et al. (2011) have used a low-dimensional representation of connectivity differences obtained from non-parametric hypothesis testing and linear discriminant analysis to classify Alzheimer's disease patients, MCI patients, and normal subjects. To our knowledge, however, no multivariate predictive modeling approach based on functional connectivity has been reported in MS.

Here, we describe a functional connectivity analysis of resting state data adapted from our recently developed multivariate connectivity decoding technique (Richiardi et al., 2011), which we use to discriminate between minimally disabled MS patients (median EDSS 2.0) and healthy controls, a first step towards the development of predictive prognosis models. Our approach exploits whole-brain data rather than restricting the study to a few regions of interest such as motor cortices or the DMN. By doing so, we aim at exploring global connectivity changes in MS and defining which functional connections are particularly affected by the disease. Beyond the data-driven exploration of the functional impact of distributed connectivity damage associated with MS, our method provides a classifier model that gives predictive information on individual status (as opposed to whole-group analysis based on a priori classification). The ability to classify patients based on fMRI connectivity patterns is a first step towards developing useful tools for improving the diagnostic workup and the monitoring and prognosis of MS patients, even in the absence of overt clinical signs or visible structural lesions.

Materials and methods

Subjects and task

Twenty-two relapsing–remitting (RR) MS patients according to McDonald's diagnostic criteria (Polman et al., 2005) were selected from our outpatient clinic database. The selection criteria were (1) mild to moderate neurological disability but unimpaired ambulation (Expanded Disability Status Scale (EDSS) ≤ 2.5 in all cases; Kurtzke, 1983); (2) no clinical relapse and no corticosteroid therapy for at least 6 weeks before inclusion in the study; and (3) no other neurological diagnosis, major depression, or psychiatric illness according to the DSM-IV criteria. All underwent a similar MRI protocol during their follow-up, with all parameters of the imaging sequence equal and with the same MRI scanner in all subjects, in order to prevent confounding factors in the analysis. All patients were only minimally disabled (median EDSS 2, range 1.5–2.5), with five subjects having had a single attack at the time of imaging. At the time of scanning, 11 out of 22 patients were receiving disease-modifying therapies (interferon β-1a or 1b in nine cases, glatiramer acetate in two cases) for a mean duration of 38.8 ± 37.1 months).

The control group consisted of 14 healthy subjects with no history of alcohol or drug abuse, major psychiatric disorder (major depression, psychosis, untreated bipolar disorders), head trauma, other neurological disorder, or systemic illness.

The characteristics of the study population are summarized in Table 1, and full details are provided in Supplementary Table 1.

The study was approved by the local university ethics committee, and all subjects gave informed consent for their participation in accordance with the Declaration of Helsinki.

Data acquisition

Data was acquired on a Siemens 3 T TrioTIM (VB15) platform, using a 32-channel head coil. Functional imaging data were acquired in one session using gradient-echo echo-planar imaging (TR/TE/FA = 1.1 s/27 ms/90°, matrix = 64×64, voxel size = $3.75 \times 3.75 \times 5.63$ mm^3, 21 contiguous transverse slices, 450 volumes). Longitudinal magnetization was assumed to reach steady state after approximately 10–11 s, and the first 10 scans of each acquisition were discarded. In total, $T = 440$ volumes were kept for analysis. The resting state scanning took 8 min. Participants were instructed to lie still with their eyes closed to relax and let their mind wander without doing anything in particular (as is standard practice in resting state fMRI studies; Fox and Raichle, 2007; Mantini et al., 2007; Helekar et al., 2010).

A structural image was also acquired using a high-resolution three-dimensional T1-weighted MPRAGE sequence (160 slices, TR/TE/FA = 2.4 s/2.98 ms/9°, matrix = 256×240, voxel size = $1 \times 1 \times 1.2$ mm^3).

In addition, a turbo spin-echo proton density (PD) image (46 slices, TR/FA = 2640 ms/150°, matrix = 204×256, voxel size = $0.98 \times 0.98 \times 3$ mm^3) was acquired for lesion tracing.

Data processing and construction of the functional connectivity matrix

Lesion masks and lesion load computation

Lesions were traced manually on the PD image by two independent radiologists (Medical Image Analysis Center, University Hospital Basel, E.W. Radue). Lesion load was calculated by multiplying the total number of traced lesion voxels by the voxel volume.

Table 1
Demographic information of the study population.

	Patients ($n = 22$)	Controls ($n = 14$)
Gender (M/F)	8/14	5/9
Mean age at inclusion (SD)	36.8 (7.9)	38.4 (6)
Median EDSS (range)	2.0 (1.5–2.5)	–
Mean years of disease duration (SD)	4.7 (3.5)	–

Structural and resting state data

To extract the resting state functional connectivity matrix, we follow the methodology described in previous work (Achard et al., 2006; Richiardi et al., 2011). Supplementary Section 1 provides an overview of the processing pipeline.

For each subject, the functional data is spatially realigned and motion-corrected to the mean image with SPM8 (least square technique with rigid body and quadratic interpolation). Movement parameters are checked for excessive translation and rotation, and the volumes were inspected visually for intensity spikes, which are due to the spin-history effect in case of large movement (Friston et al., 1996). One patient (not included in Table 1) was excluded due to excessive movement.

Each subject's structural image is normalized to MNI space and segmented using the SPM8 (http://www.fil.ion.ucl.ac.uk/spm/) *new segmentation* algorithm, an updated version of the unified segmentation algorithm (Ashburner and Friston, 2005). The structural image is co-registered to the mean image of the functional data. An individual brain atlas containing 90 cortical and sub-cortical regions of interest (ROIs) is then computed with a modified version of the IBASPM toolbox (Alemán-Gómez et al., 2006) and the AAL atlas (Tzourio-Mazoyer et al., 2002). A full list of these regions is provided in Supplementary Table 2. This structural atlas is then mapped back onto the native resolution of the functional data, the time series are linearly detrended, and region-averaged time series are obtained. These regional time series are windsorized to the 95th percentile to increase robustness to outliers. At this stage, each subject's functional data is contained in a $90 \times T$ matrix (multivariate time series).

The regional time courses are then filtered into frequency subbands using a wavelet transform (cubic orthogonal B-spline wavelets). The subband of interest for this study contains frequencies in the 0.06–0.11 Hz range, to focus on resting state activity (Richiardi et al., 2011). While the commonly used frequency band is wider (Biswal et al., 1995; Lowe et al., 1998), the use of wavelet correlation (Achard et al., 2006) relies on a dyadic wavelet decomposition, where the influence of boundary conditions becomes more important as we move to coarser (lower frequency) subbands. Given the available acquisition time, the current subband is theoretically a good compromise between boundary condition artifacts (getting worse towards lower frequencies because there are fewer independent samples) and signal-to-noise ratio (getting worse towards higher frequencies because of the hemodynamic response acting as a low-pass filter). To further ensure that the time course noise (due to movement or scanning artifacts) does not add a confound and is equal between control and subject groups, the average standard deviation of the regional filtered time courses $\bar{\sigma}_R$ is computed for each subject, and a Kruskal–Wallis test is conducted on the hypothesis of no difference in median value of $\bar{\sigma}_R$ between groups.

After computing pairwise Pearson correlations between all ROIs in the atlas, a 90×90 correlation matrix is obtained for each subject. Note that for the whole procedure, the data of each subject is not influenced by the data of other subjects; e.g., no groupwise registration is used. This will ensure independence later on in the modeling stage and allows a proper deployment of predictive approach.

Modeling and classification of connectivity matrices

The functional connectivity matrix can be considered as the *adjacency matrix* of an undirected, weighted, complete graph by removing the diagonal elements. This defines the *connectivity graph*, where each atlas ROI corresponds to a vertex and the strength of functional connectivity between two ROIs is encoded in the edge weight (a correlation coefficient). To permit the use of machine learning algorithms,

we use the direct graph embedding method (Richiardi et al., 2010), in which the upper triangular part of the adjacency matrix is lexicographically organized in a vector representation. This provides a flexible approach enabling us to model the whole-brain graph, or to examine a specific hemisphere or lobe, or even to consider connections inside functionally defined networks. These types of subgraphs can be readily extracted from the full adjacency matrix and represented as vectors. It is possible to train the classifier on the whole graph and then to study the relative discriminative importance (weights, see below) of various subgraphs or to directly train the classifier on subgraphs. In the remainder of this work we focus on the former method. Thus, at this stage, each subject's resting state data is represented by a feature vector whose elements are pairwise regional correlation coefficients. We point out that the input features used in Craddock et al. (2009) are equivalent to our direct embedding approach, the difference being the addition of a Fisher R-to-Z transform step and the lower dimensionality of the feature space generated (15 regions lead to 105 edge weights in feature space).

For classification, we use an ensemble of functional trees (Richiardi et al., 2011), a variation on the random forest scheme occasionally used in neuroimaging (Langs et al., 2011). This classifier yields a *discriminative weight* w_i for each functional connection in our resting state data. This value represents the relative ability of each connection to discriminate between controls and MS patients. Their interpretation is very close to that of regression coefficients, except that they only make sense as part of a multivariate pattern: connections with high discriminative weight are useful in predicting patient status (they are a good predictor), while connections with low discriminative weight carry little information. After permutation testing to remove connections with insignificant discriminative weights, the set of remaining connections yields what we call a *discriminative graph*. The discriminative weight of each connection can then be used to compute *regional discriminative weights* by summing the discriminative weights of all connections attached to a particular region. The regions and connections of the discriminative graph can be represented in MNI space. By visualizing the connections and regions that are jointly most discriminative (those from which a prediction of the MS status of any new subject can be made), we can obtain a map of all connections driving the classification between patient and control groups. Supplementary Section 1.4 contains more details about the computation of discriminative weights, including the permutation testing approach used for statistical control.

In order to evaluate the performance and generalization ability of the classifier, we adopt a leave-one-subject-out cross-validation approach, whereby the dataset is split N times into a training set containing $N-1$ subjects and a test set containing one subject. The training set is used for learning the classifier parameters, while the held-out testing set is used for prediction. We can then measure how well the classifier is performing by aggregating prediction results across the cross-validation folds.

We report the classification performance using the familiar measures *sensitivity* and *specificity*. Supplementary Section 7 contains more details about the computation of performance measures.

Summary indices of connectivity alterations

We can divide the set of connections C that provide discrimination between controls and MS patients into two distinct, non-overlapping parts: connections that are, on average, weaker in patients than in controls (C_-), and those that are stronger (C_+). Thus, we have $C = C_- \cup C_+$ and $C_- \cap C_+ = \varnothing$. Then, we can compute two summary measures per subject, which can serve for post hoc comparison of the results between groups.

For each subject s, the *increased connectivity index* (ICI) is the sum of correlation values of the connections in C_+, denoted ρ_i^s, each multiplied by its normalized discriminative weight $\hat{w}_i = \frac{w_i}{\|\mathbf{w}\|_1}$. Thus, we have $ICI^s = \sum_{j \in C_+} \rho_j^s \hat{w}_j$. The *reduced connectivity index* (RCI) is computed in the same way, but from the set of connections that are weaker in patients, C_-; that is for each subject, $RCI^s = \sum_{j \in C} \rho_j^s \hat{w}_j$. These two different indices can be plotted jointly to provide a simple two-dimensional view of discriminative connectivity alterations in MS patients with respect to controls, e.g., subject 4 would be plotted in $\mathbb{R}^2$ as (RCI^4, ICI^4). Fig. 1 of the results section provides an example.

Additionally, for statistical analysis we may want to remove the bias due to total edge strength of the connectivity graph (sum of edge weights $\sum_i \rho_i^s$), which can vary considerably between subjects, and we can compute the normalized RCI, respectively ICI, as $nRCI^s = \frac{1}{\sum_i \rho_i^s} RCI^s$. This reflects the discriminative importance and connection strength in the discriminative (sub)graph with respect to the total edge strength of the connectivity graph.

These indices are different from a simple averaging of correlation values, because only a discriminative subset of connections is used, and the sum is weighted by the discriminative importance of each connection. We should also point out that Chen et al. (2011) have previously defined a “decreased connectivity index” and an “increased connectivity index”. While related to our ICI and RCI, these are different from our indices. They are computed from an “increased connection set” (respectively decreased), which is the set of connections whose z-scores, obtained from a Wilcoxon rank-sum test between groups, are the n most positive (respectively negative). Within the increased (respectively decreased) connection set, the correlation values are averaged, forming the indices. Furthermore, they are used as input features to an LDA classifier in that paper, as opposed to being a post hoc summary measure of a high-dimensional discrimination function in our approach.

Results

Predictive modeling of whole-brain resting state functional connectivity patterns has high sensitivity for MS

The pattern of correlation coefficients between all pairs of ROIs was calculated for each subject in the MS and control groups and submitted to our multivariate decoding algorithm to determine the most consistent differences in the low-frequency functional connectivity in resting state between the two groups.

After cross-validation, 18 out of 22 patients and 12 out of 14 controls were classified correctly. These results correspond to a sensitivity of 82% (above chance at $p<0.005$, Wilson's method for the binomial distribution) and a specificity of 86% (above chance at $p<0.01$). Importantly, these classification results are not driven by noise differences between patients and controls, as indicated by calculating the standard deviation of the regional filtered time courses $\bar{\sigma}_R$ ($p=0.24$, Kruskal–Wallis test on the null hypothesis of no difference in median value of $\bar{\sigma}_R$ between groups).

When looking at the misclassified patients (details in Supplementary Table 1), it can be seen that two of them had only a single attack preceding their inclusion in our study and a lesion load in the lowest quartile of our sample (0.39 and 0.51 cm^3). The two other misclassified patients had an EDSS score of 1.5, i.e., the lowest in our database. This suggests that a potential source of classification errors might concern the minimal disability caused by the disease when lesion load still has little or no impact on global functional connectivity. Regarding patient treatment, it seems to have no effect on the performance of the classification algorithm, but the sample size is not sufficient to assert this with confidence.

Fig. 1 shows the scatterplot of the increased and reduced connectivity indices (ICI and RCI) computed post hoc on the whole group (see method described in Section Summary indices of connectivity alterations). This representation, where each index is based on a distinct sub-network of the discriminative graph, reveals good separation between the groups. This suggests that the discriminative graph can indeed successfully capture a predictive subset of

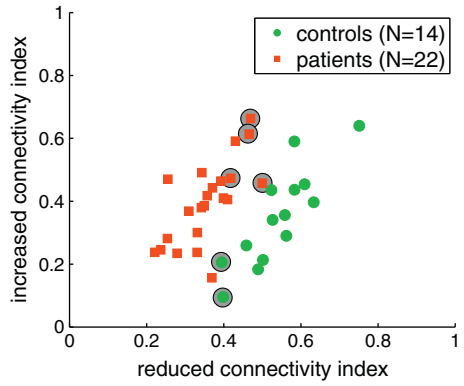

Fig. 1. Scatterplot of reduced and increased connectivity indices for controls (green circles) and patients (red squares). This is a summary representation of the pattern of connectivity alterations that is predictive of MS in our sample, computed post hoc on the whole dataset. Points corresponding to subjects misclassified by our decoding algorithm in the leave-one-out cross-validation procedure are circled in gray.

connections and that the discriminative weight is reliably estimated across different subjects. As shown in this figure, misclassified patients are generally in the region of the RCI/ICI graph corresponding to high connectivity for patients, both in the C_- and C_+ subnetworks. This entails these patients tend to exhibit stronger connectivity with respect to controls than the classifier expected from the training sample. Likewise, the misclassified controls tend to be those with the weakest connectivity in both the C_- and C_+ subnetworks.

Interestingly, there is a significant positive correlation between nRCI (see Section Summary indices of connectivity alterations) and the lesion load computed in MNI space (robust correlation coefficient; Rousseeuw and Driessen, 1998: 0.61; IRWLS robust linear regression: $p<0.001$ to reject the null hypothesis of a zero slope coefficient). This suggests that, while total edge strength ($\sum_i \rho_i^s$, computed over the whole connectivity graph for each subject) might not be a good indicator of lesions (non-significant correlation between the vector whose elements are the total edge strengths from all patients and the vector whose elements are the corresponding lesion load values from all patients), the effect of white matter lesion can be observed within a small subgraph (part of the discriminative subgraph) learned on resting state connectivity, linking known physiological effects of the disease with functional MRI connectivity measurements. Indeed, this finding may be taken as evidence that discriminative functional connectivity changes can at least partly be attributed to white matter lesions. Furthermore, although no causal mechanism is clear, this may indicate that connectivity strength of the C_- subgraph relative to the rest of the network is increased in these minimally disabled patients in an effort to compensate for increasing lesion load, while still being below the connectivity strength of controls.

Supplementary Table 4 contains the weight of all connections that make up the two indices. For an anatomical representation of subgraphs corresponding to the ICI and RCI, see Fig. 4.

Connections distinguishing MS from controls at rest form a large-scale network with low edge density

To visualize the anatomical organization of connectivity changes (see Section 1.4), we first extract the *discriminative graph* indicating which connections and regions are jointly most discriminative between controls and MS patients. In this sample we find 161 connections (out of 4005) that have significant discriminative weights ($p<0.05$, corrected for multiple comparisons by permutation testing), corresponding to an edge density (connectance) $\mathcal{D}=\frac{161}{4005}\approx 0.04$. Since $\mathcal{D}\ll 1$, we interpret the discriminative graph as having a low edge density. The connections with significant discriminative weights are shown in Fig. 2. The size of the ROIs spheres and connection paths is proportional to the number of times a connection to or from a region is selected for classification during cross-validation and how discriminative it is between the groups. Note that since the method is multivariate, these connections are not discriminative on their own, but rather, the joint set of connections is discriminative.

The overall pattern of changes reveals a network of functional connections mainly centered on subcortical and fronto-parieto-temporal regions, consistent with the typically widely distributed lesions in MS. However, different patterns can be seen in different parts of the brain. A notable feature is that occipital regions are not particularly important in the differentiation of MS from control brains, even though visual networks often constitute a distinctive component of resting state activity in normal conditions (Mantini et al., 2007; Raichle et al., 2001; Salvador et al., 2005). The frontal lobe contains relatively few connections with high discriminative weight, both long range and short range. More remarkably, the temporal lobe and subcortical gray nuclei contain a few important hubs showing marked changes in connectivity between patients and controls.

The discriminative power of each individual lobe is summarized in Fig. 3 (left), with separate plots for within-lobe and between-lobe connections. As can be seen, discriminative connections are predominantly inter-lobe, but intra-lobe connections are equally or more important for temporo-parietal regions. The latter typically correspond to long range pathways in posterior-anterior axis along the periventricular regions. Connections to and from subcortical regions are also particularly discriminative, highlighting the widespread connectivity of these structures.

Because inter-hemispheric connections are likely to rely on the corpus callosum, which is a known location for MS lesions (Compston and Coles, 2008; Noseworthy et al., 2000; Rocca et al., 2007), it is of particular interest to separate the discriminative graph into ipsi- and contra-lateral subgraphs (C_I and C_C). Inspection of the discriminative graph in Fig. 2 suggests that some connections with contralateral areas may have larger discriminative power (a detailed subdivision is available in Supplementary Fig. 3). This is confirmed ($p\ll 0.01$ and generalized $\eta^2=0.8$) by a repeated measures ANOVA testing the effect of grouping by subgraphs C_I or C_C on the sum of significant discriminative weights in each cross-validation folds. Nevertheless, it should be noted that there clearly is a large amount of discriminative information in the ipsilateral subgraph as well. This implies that the functional connectivity at rest is altered by MS both within and between brain hemispheres, and that both types of changes are reliable indicators of the disease.

Moreover, at detailed look at connections across lobes reveals a subtler picture: when the discriminative weights of each lobe are divided into ipsi- and contra-lateral parts (Fig. 3, right part) the temporal lobe shows the most predictive differences for inter-hemispheric connections, whereas limbic structures (cingulum, hippocampus and parahippocampal formation, and amygdala) and the insula only show alterations in intra-hemispheric functional connectivity. Parietal and frontal lobes seem to have an equal balance of discriminative weight between inter- and intra-hemispheric connections.

Finally, it is also important to distinguish between increases and decreases in connectivity. When examining the whole network, we found that discrimination is mostly driven by connections that are on average stronger in controls, suggesting a characteristic reduction of functional connectivity in patients. However, there is a set of ROIs where some connections with other areas show increased connectivity in patients. Fig. 4 shows a division of the discriminative graph into a subnetwork with increased connectivity in patients with respect to controls (C_+) and vice versa (C_-). It is apparent that the regions involved in C_+ form a network whose main connections link the thalamus to medial and anterior temporal pole, mainly contralaterally (with stronger effects for the right hippocampus, right amygdala, and bilateral temporal poles). Connections are also heightened between the right amygdala, right hippocampus, and right temporal

pole. Several connections to and from the left parahippocampal regions are also stronger in this network. Supplementary Fig. 2 shows the relative discriminative weight of some of these connections. These increases of connectivity in MS patients therefore appear much more circumscribed than decreases, which are observed for long-range pathways both within and across hemispheres.

Connections outside the default mode network are also informative

Studies have highlighted alterations to the DMN (Buckner et al., 2008) associated with multiple sclerosis (Bonavita et al., 2011; Roosendaal et al., 2010). To investigate this effect more specifically in our data, a subnetwork of the whole-brain graph comprising regions that are part of the DMN was defined (based on the work of Buckner et al., 2008), and including the ventral and medial prefrontal cortex, the posterior cingulate and retrosplenial cortex, inferior parietal lobule, lateral temporal cortex, and hippocampal formation (details are in Supplementary Table 3). The discriminative weight of connections within the default mode network was tallied separately from the discriminative weight of connections to the outside of the default mode network.

Results are summarized in Fig. 5, clearly showing that discriminative changes do not only affect connections between DMN regions, but also connections between DMN regions and the rest of the brain. In fact, more discriminative information is contained in regions that are not part of the DMN, highligthing the interest of examining whole-brain networks. Remarkably, however, the region with the highest discriminative weight, the right middle temporal pole, is part of the default mode network. Moreover, several DMN regions, such as the left precuneus, the bilateral superior frontal orbital cortex, and the right anterior and posterior cingulate cortex, exhibit more discriminative connections to and from the DMN than to and from the rest of the brain. This is consistent with the existence of a specific functional architecture of the DMN that is disrupted by MS pathology.

Discussion

The present study shows that a multivariate approach based on predictive modeling of brain connectivity at rest allows a reliable differentiation of minimally disabled multiple sclerosis patients and healthy control subjects. Our results do not only confirm that functional changes affecting widespread (cortical and subcortical) networks are a prominent feature of MS brain pathology (Miller et al., 2003) but also show that these alterations can be reliably and sensitively measured using functional MRI of resting state, and furthermore be used to classify disease state in individual subjects. Our method is based on an established technique of brain decoding using wavelet decomposition of resting state time courses (Eryilmaz et al., 2011; Richiardi et al., 2011), previously applied to study cognitive and emotional states in normal conditions, but adapted here to assess pathological states.

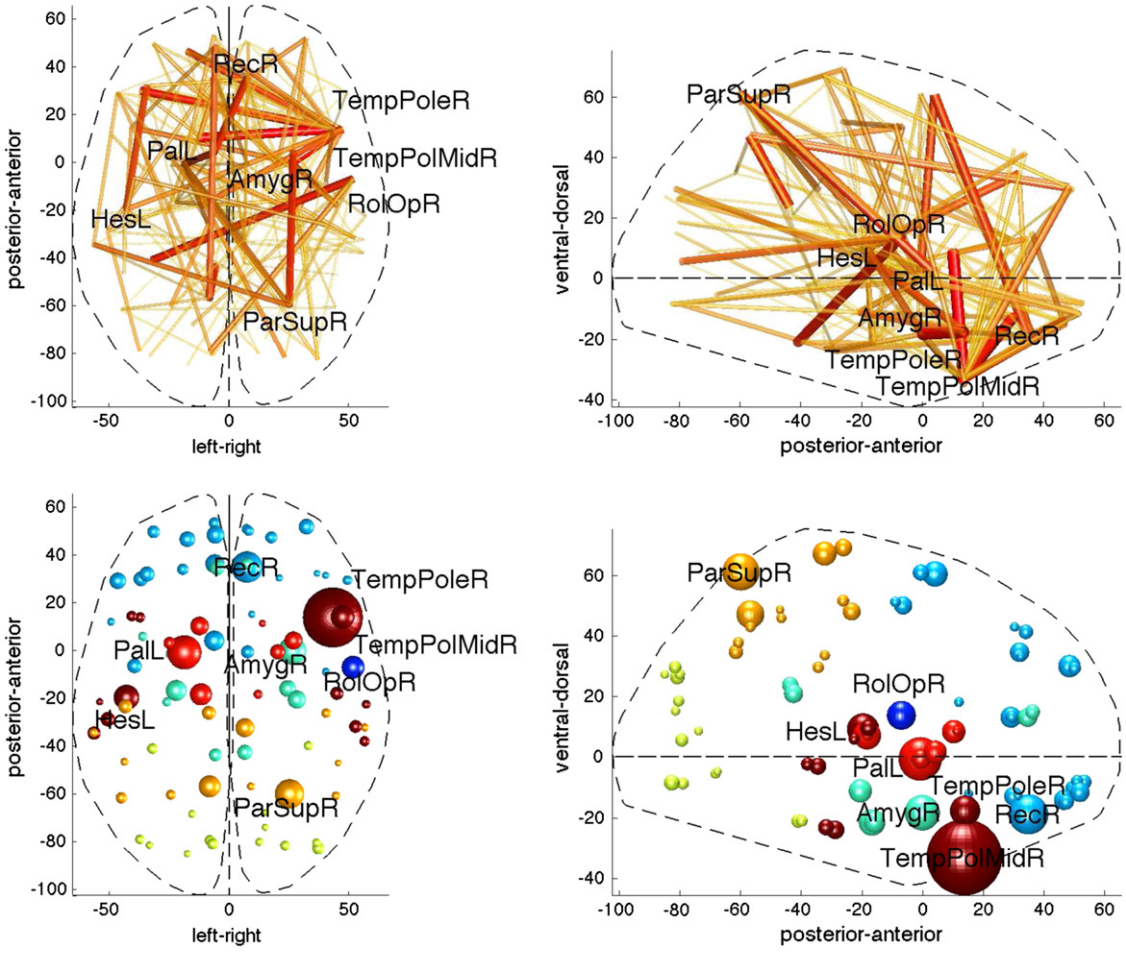

Fig. 2. Anatomical illustration of discriminative graphs for MS versus control subjects. In the top row, the size and shade of connections between regions reflects their discriminative weight: stronger hues and larger sizes reflect higher discriminative weight. In the bottom row, the size of each sphere depicting an atlas region is proportional to its regional discriminative weight (sum of the discriminative weights of all connections between this region and the rest of the brain). Color indicates the lobe where each region is located (dark red = temporal, clear blue = frontal, yellow = parietal, green = occipital, cyan = limbic structures (cingulum, hippocampus and parahippocampal formation, amygdala) and insula, clear red = subcortical gray matter). Name labels are given for the regions with the highest regional discriminative weights (limited to 8 for clarity).

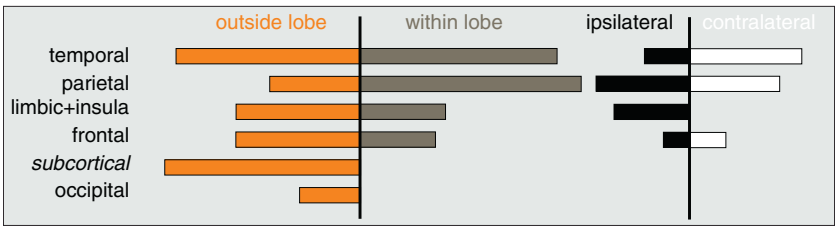

Fig. 3. (left graph) Summary of discriminative weights of ROIs by lobe, distinguishing connections that link to other regions outside the lobe from connections that stay within the same lobe. The lobes are ordered from overall most discriminative to overall least discriminative. Limbic structures include cingulum, hippocampus and parahippocampal formation, and amygdala. (right graph) Further subdivision of within-lobe connections into ipsilateral and contralateral connections.

Used rigorously, classifiers in a pattern recognition approach provide very powerful tools to explore high-dimensional data and to capture consistent but unknown features, without limiting the findings to specific hypotheses. Our results take into account the full high-dimensional data consisting of 90×90 connections, but the discriminative graphs showing the distinctive functional connections are readily interpretable and the results can even be summarized by two principal measures: the reduced connectivity index (RCI) and the increased connectivity index (ICI), which reflect the main characteristics of connectivity alterations. Furthermore, by using a leave-one-subject-out cross-validation technique, the results have shown the applicability of our method to single subjects. With important caveats, the performance obtained with the proposed method can be compared with the results of Weygandt et al. (2011), based on a searchlight approach to structural T2-weighted images. In particular, their larger study population is in generally worse condition (longer average disease duration, larger EDSS range; maximum: 7) and their analysis uses the cerebellum as well. While the best performance (96% leave-one-out balanced accuracy) is obtained using hand-segmented lesion masks, the analysis of normal appearing gray matter yields up to 82% balanced accuracy, and normal appearing white matter yields up to 91% accuracy. Our results, at 84%

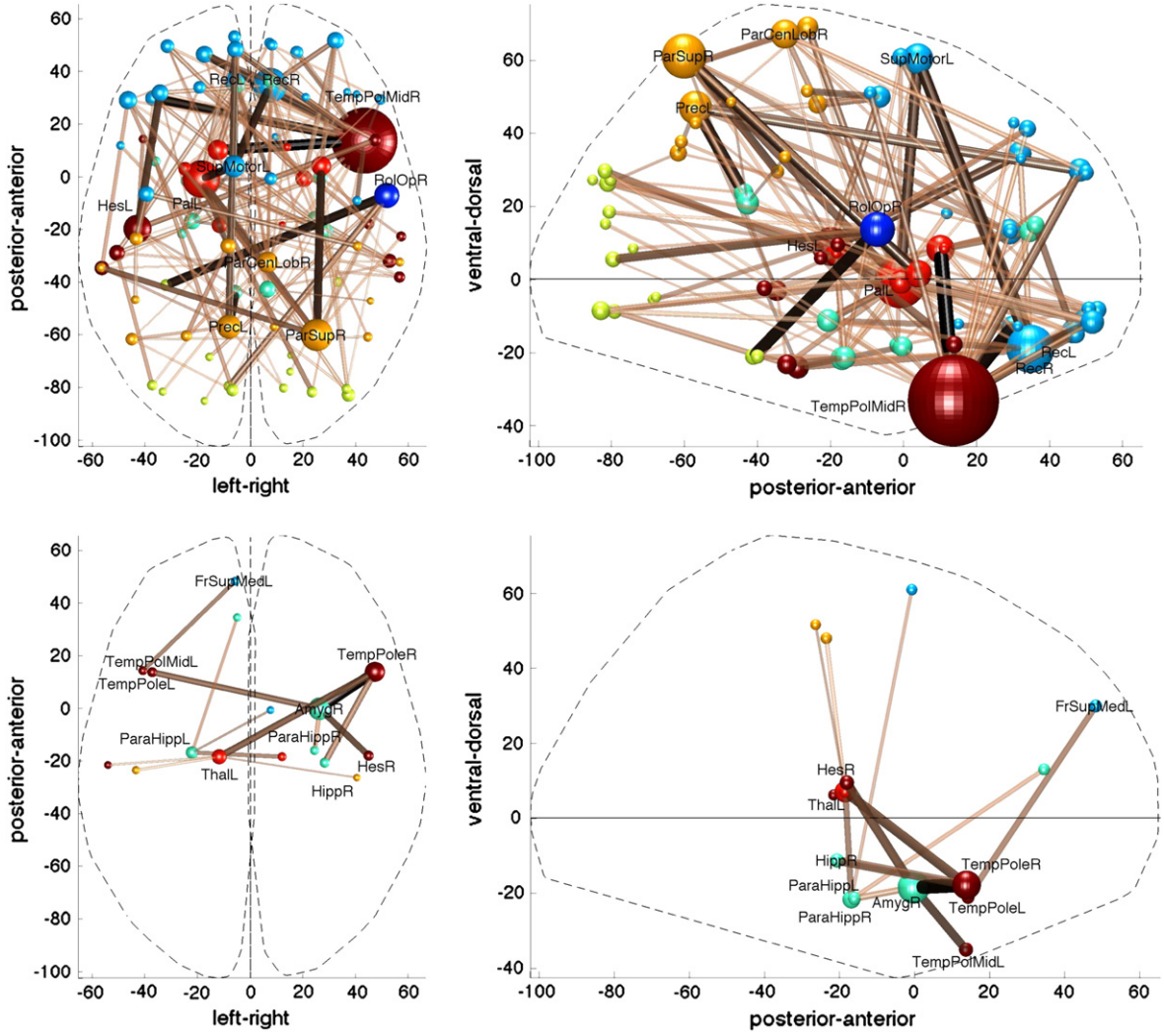

Fig. 4. (top) Subnetwork where patients have on average weaker connectivity than controls (C_-). (bottom) Subnetwork where patients have on average stronger connectivity than controls (C_+). The size and shade of connections between regions reflects their discriminative weight: stronger hues and larger sizes reflect higher discriminative weight. The size of spheres for atlas regions is proportional to its regional discriminative weight Color indicates the lobe each region is part of (see Fig. 2 for the color coding).

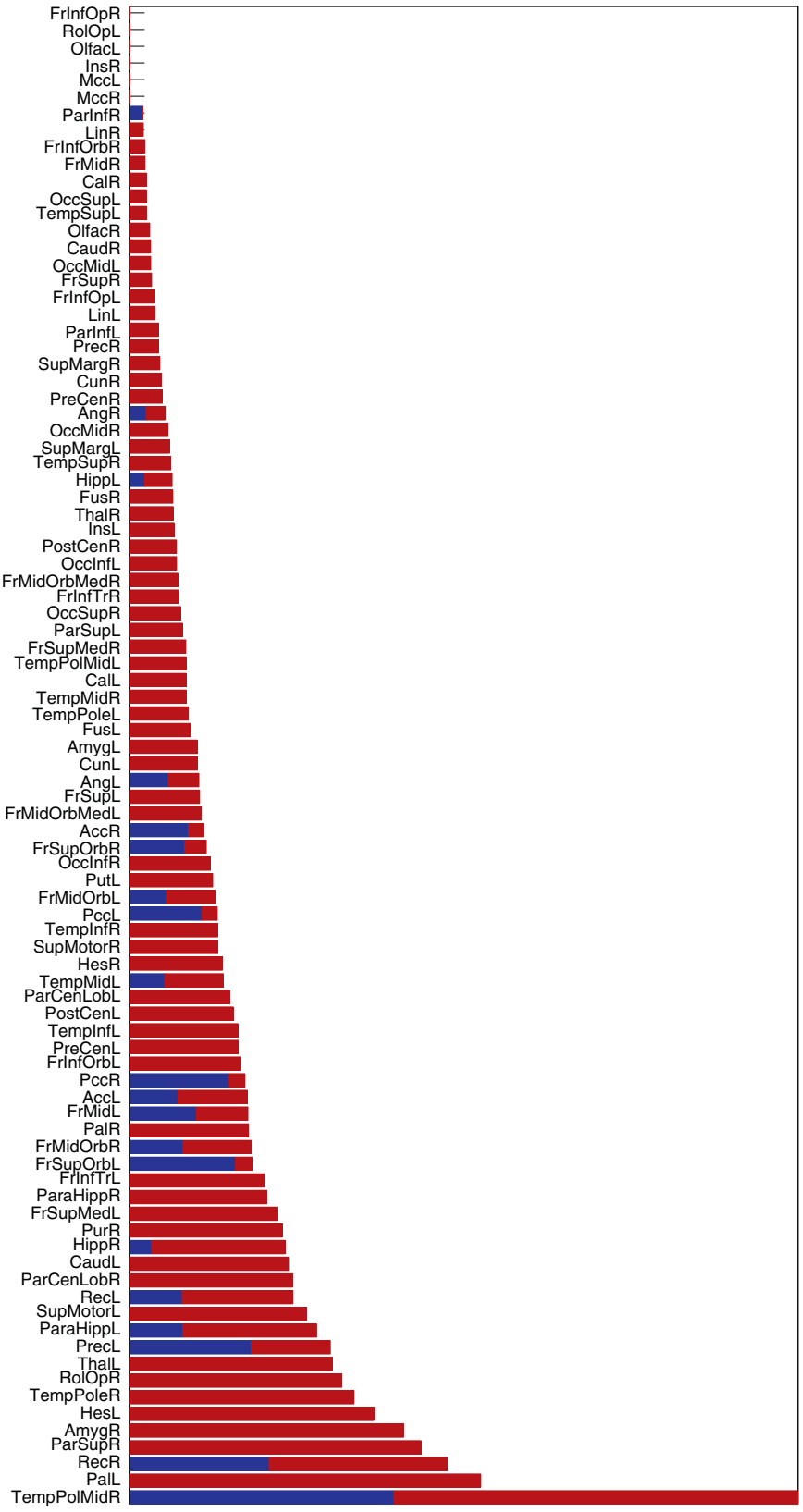

Fig. 5. Regional discriminative weights divided into connections within (blue, close to axis) and outside (red, away from axis) the DMN.

balanced accuracy, can therefore be considered encouraging since no cerebellum is used in our study, and the population is minimally disabled. Furthermore, subtle white matter alterations, to which our technique is sensitive, seem to be in and of themselves discriminative, which hints at possible future gains in accuracy by refining our method. However, and despite their statistical significance, our current sensitivity and specificity figures must still be taken with caution because of our limited sample size. MS is a heterogeneous disease, and

our leave-one-out results offer only limited evidence of generalization ability to a separate cohort.

Many other analyses of resting state in neurological diseases concentrated on the default mode network (DMN) or focused on a small number of regions, for example, by using univariate methods to compare the goodness of fit of patients and controls to a standard DMN template (Greicius et al., 2004) or by measuring the cross-correlation coefficient of activity over time for a single region (Li et al., 2002). In MS, some studies (Lowe et al., 2008) explored functional connectivity only to and from motor areas and did not find significant whole-group difference between minimally disabled MS patients and healthy controls. Moreover, many of the few studies addressing resting state alterations in MS concentrated only on the DMN (Bonavita et al., 2011; Rocca et al., 2010). However MS lesions are not restricted to the DMN. Our results show that the connections within DMN regions are affected but do not represent the only nor the most common ones contributing to correct classification. The major advantages of our multivariate approach, taking into account connectivity across the entire brain, include a greater versatility and a higher sensitivity, two crucial features for discriminating different conditions and studying early stages of pathology. Whole-brain analysis using ICA in MS has indeed been reported to bring out significant differences between groups in various brain networks apart from the DMN Roosendaal et al. (2010). Additionally, the good performance of using multivariate methods with whole-brain functional data to derive imaging markers has also been reported in other pathologies, for example depression (see, e.g., Greicius et al., 2007; Craddock et al., 2009) or Alzheimer's disease (see, e.g., Buckner et al., 2009; Chen et al., 2011).

Overall, our data indicate that only about 4% of the total possible connections considered in our study (between the 90 ROIs distributed over the entire cortex and subcortical nuclei) are discriminative between minimally disabled MS patients and healthy controls. Thus, the large majority (i.e., the remaining 96%) of functional connections have non-significant discriminative weights. However, these 4% still represent numerous (161) connectivity pairs. Although there is no single pathognomonic path affected by MS (consistent with widely distributed lesions (Compston and Coles, 2008; Polman et al., 2011), these altered connections are not uniformly distributed across the brain and specific patterns are visible. Below, we discuss the possible significance of these changes.

Topology of the discriminative connections

The discriminative connections between all ROIs considered were located throughout the brain, including in particular the temporal lobes (with a predominance for the right temporal pole), the superior parietal lobes, as well as the frontal lobes and some limbic structures, plus several structures among subcortical gray nuclei. Strikingly, in contrast, the connections concerning the occipital lobe had very low discriminative weight, although clinically MS often presents with visual disturbances (Compston and Coles, 2008; Noseworthy et al., 2000). However, the latter are typically related to an early affection of optic tracts (Ciccarelli et al., 2005; Dineen et al., 2009; Reich et al., 2009), which was not specifically investigated here.

The discriminative connections were mostly associated with long-range pathways presumably grouped around the ventricles for intra-parietal and intra-temporal pairs or centered on inter-hemispheric pathways for parieto-parietal and temporo-temporal connections. Frontal and limbic connections were also affected but to a lesser extent. This observation converges with the preferential location of MS lesions in areas of dense venular distributions, i.e., around the lateral ventricles, and at the cortico-subcortical junction (Compston and Coles, 2008). In addition, the connectivity of deep gray matter nuclei (thalamus and basal ganglia) was also markedly affected, which is consistent with the fact that these subcortical nuclei both receive and project to large parts of the neocortex and that many of these projections also travel in periventricular white matter (e.g., thalamic radiations).

Notably, among connections with significant discriminative weight across the whole brain, we found that inter-hemispheric connections are more discriminative than intra-hemispheric connections, even though the latter still make an important contribution to discriminative power. This finding is compatible with the well-known preferential affection of the corpus callosum in MS (Evangelou, 2000; Gean-Marton et al., 1991; Mesaros et al., 2009; Rocca et al., 2010; Yaldizli et al., 2011) and presumably reflects in part the concentration of all inter-hemispheric connections at a relatively small circumscribed location in the brain. Our results therefore add to previous studies reporting a decreased inter-hemispheric functional connectivity at rest in MS patients (Cover et al., 2006). However, our data also go beyond these studies by demonstrating that such decreases are not specific to inter-hemispheric connections, since most of the functional connectivities with a significant discriminative weight are decreased in patients, both within and between the two hemispheres. As a particular case, we found that inter-hemispheric connections in limbic structures (cingulum, hippocampus and parahippocampal formation, and amygdala) and the insula provide no discriminating information about patients and controls. Taken together, these findings highlight the importance of considering intra-hemispheric connections when analyzing functional connectivity in MS, even in resting state conditions. We cannot exclude the possibility, however, that the relatively high significance of intra-hemispheric pathways (compared to inter-hemispheric pathways) may reflect the minimal disability in our patients, given the known association between callosal atrophy and disease progression (Pelletier et al., 2001).

Several of the relatively most discriminative connections were centered around the right temporal pole — including left caudate to right middle temporal pole, right amygdala to right temporal pole, left inferior frontal orbital to right middle temporal pole, and left superior frontal orbital to right middle temporal pole. However, it must be kept in mind that these pairs represent only the top of 161 discriminative connections that all together are responsible for multivariate pattern classification and that none of these connections is significantly discriminative on its own. Looking for a more synthetic view, a region that is part of several discriminative connection pairs becomes a discriminative region itself. Under this measure, the most discriminative regions were located in the anterior right temporal lobe, but also in the bilateral superior parietal lobes, orbitofrontal cortex (gyrus rectus), left globus pallidus, and right amygdala. An alteration of the underlying structural connectivity (due to white matter injury) is likely to account for the important impact of MS on a few specific regions such as the temporal pole or pallidum, as these regions are known to constitute strong hubs in brain connectivity (Haber and Knutson, 2010; Olson et al., 2007). In particular, the temporal poles are densely connected to orbito-frontal cortex (via the uncinate fasciculus), amygdala, temporal and occipital ventral regions (via the inferior longitudinal fasciculus), as wellas the temporo-parietal junction, and as such constitute high-level associative cortical areas integrating deeply processed information from various parts of the brain (Olson et al., 2007). By being somewhat at the "top of processing hierarchy," these temporal areas might reflect a common impact of disrupted connectivity in widespread pathways throughout the brain.

We also note that many functional connections highlighted by the present approach may not necessarily imply the existence (or damage to) direct structural connections. In fact, coherent activity between distant areas might be subserved by either direct white matter pathways or more global synchronization processes involving other nodes in a common networks and/or diffuse projections from subcortical (e.g., brainstem) structures (see Golanov and Reis, 1996, for an example in the rat). These more global influences might account for connections found across non-homologous areas between the two hemispheres. While our methodology cannot distinguish between structural and non-structural sources of functional connectivity, it is likely to gain

higher sensitivity by measuring the impact of diffuse lesions that may affect both types of connections.

Decreased and increased connectivity in MS patients

Most of the significant connectivity changes reflected decreases in patients compared to controls, consistent with an impaired functional coupling between distant brain areas due the presence of MS lesions. However, there were also a few connections showing increased strength in MS compared to controls. These connections were found in a specific subnetwork, roughly consisting of bilateral and interhemispheric connections around the thalami, medial temporal areas (para-hippocampal gyrus, amygdalae), and temporal pole. An increase in low-frequency activations (not connectivity) in the thalamus, insula, and superior temporal gyrus has previously been reported in MS (Liu et al., 2011) and interpreted as compensatory plasticity. Here, however, we did not find changes in insula connections allowing a reliable group discrimination, but the insula is also known to be connected to the temporal pole and amygdala (Augustine, 1996).

Note that our method is sensitive to both reduced and increased connectivity without any a priori. Increased connectivity (reflected in the ICI values) by itself is however not a discriminating feature between patients and controls, because information about increased connectivity is significant only together with the concomitant reduction in connectivity (reflected in the RCI). Nevertheless, in our data, the strongest distinction between subjects and controls is provided by the RCI, and considering only the sum of correlations for reduced connections (projection on the RCI axis of Fig. 1) still shows a reliable separation between patients and controls. This may suggest that the phenomena of decreased and increased connectivity in distinct subnetworks in MS are likely to result from concomitant but distinct factors.

The meaning of increased connectivities is not completely clear. Along with the decreased connectivities, these might reflect functional reorganization to cope with pathological damage, in keeping with results from several imaging studies in MS (Cifelli and Matthews, 2002; Hawellek et al., 2011; Mainero et al., 2004; Morgen et al., 2004, 2007; Reddy et al., 2000a; Rocca and Filippi, 2007; Trapp et al., 1998). Compensatory activation is often considered as a process arising at early stages, which tends to be lost with disease progression (Bonavita et al., 2011; Roosendaal et al., 2010). Congruent with this hypothesis, the positive nRCI correlation found with lesion loads (see Results section) seems to suggest that connectivity in the C_- subnetwork is increased to cope with lesions. However, our findings of increased connectivity in the C_+ subnetwork and increasing connectivity with lesion load in C_- might be specific to minimally disabled MS patients, a possibility that will require further testing in additional patients with more severe disease.

Note that in our study, this C_+ subnetwork predominantly concerns medio-temporal and orbito-frontal regions, normally associated with emotional processing (Kensinger and Schacter, 2008) and could therefore possibly reflect latent affective disturbances often associated with MS (Compston and Coles, 2008; Minden and Schiffer, 1990) and/or higher stress levels in patients during an MRI session (Muehlhan et al., 2011). Alternatively, we cannot exclude that the observed increases in connectivity might partly reflect stronger coherence at low frequencies due to an "idling" state of some networks at rest (Richiardi et al., 2011), subsequent to disconnection lesions in patients. Again, additional studies in patients with a broader range of MS severity will be necessary to disentangle these hypotheses.

Discriminative connections inside and outside the default mode network

Our results confirm that the default mode network (DMN) comprises many discriminative connections that are affected by MS (Bonavita et al., 2011; Rocca et al., 2010; Roosendaal et al., 2010), but they also highlight a large number of additional discriminative connections outside the DMN. Studies of resting state brain activity often focus on the default mode network because it forms a well-defined set of regions that is observed very reproducibly under different acquisition paradigms. In fact, the most discriminative ROIs in our analysis, the right temporal pole, is also part of the DMN and "consistently observed across approaches" (Buckner et al., 2008). We also found an important role for the precuneus, another core region of the DMN. In addition, we found weaker connectivity in the anterior cingulate cortex of MS patients, as reported in a previous study of resting state in MS (Bonavita et al., 2011), but an opposite effect in the posterior cingulate cortex (decreased rather than increased connectivity in patients). Nevertheless, as clearly shown in Fig. 5, many other regions that are not part of the DMN made a crucial contribution to the discrimination between patients and controls. Therefore, we conclude that resting state data analysis in MS (and other neurological conditions) should certainly comprise default mode network regions, but need not be restricted to them.

Altered connectivity and gray matter changes

The analysis of functional connectivity is based on temporal correlations of activity between gray matter ROIs. In case of decreased connectivity, it is in principle not possible to differentiate between desynchronization due to loss of white-matter pathways or gray matter pathology in one or more of the connected ROIs. Thus, functional connectivity is sensitive to both white matter and gray matter pathology and permits the investigation of both aspects of MS.

In general, MS lesions are predominantly located in white matter and therefore mainly affect axonal conduction. However, damage to cortical gray matter is also increasingly recognized (Barkhof et al., 2009; Bö et al., 2006; Prinster et al., 2006). Interestingly, our results for regional discriminative weights in different lobes show convergent patterns with what is known from anatomical studies on focal gray matter lesions (Filippi and Agosta, 2010). For instance, we found that the thalamus is involved in a high number of discriminative connections at rest. The thalamus is known to be a site of preferential atrophy in MS (Audoin et al., 2006; Cifelli et al., 2002; Wylezinska et al., 2003), possibly resulting in decreased perfusion (Rashid et al., 2004). In addition, the connections to and from several deep nuclei such as the globus pallidus, caudate, and amygdala were also discriminating between patients and controls. Early and frequent lesions in the thalamus and caudate as well as in the putamen, globus pallidus, or amygdalae have been recently pointed out (Vercellino et al., 2009), and these regions exhibit a rapid atrophy following the first clin.

Funding

This work was supported in part by Merck Serono (Merck Serono-EPFL Research Alliance Award), in part by the Swiss National Science Foundation (grant number PP00P2-123438), the Société Académique de Genève (FOREMANE fund), the Swiss Society for Multiple Sclerosis; the Center for Biomedical Imaging (CIBM) of the Geneva and Lausanne Universities, EPFL, and the Leenaards and Louis-Jeantet Foundations, and the US National Science Foundation (grant number NSF PHY05-51164).

Acknowledgments

The authors thank Prof. E.W. Radue for organising the tracing of the MS lesions at the Medical Image Analysis Center of the University Hospital Basel. We also thank Prof. R. Meuli for the scanning protocol and Michel Dreano for his comments and discussion leading up to this paper.

Appendix A. Supplementary Data

Supplementary data to this article can be found online at http://dx.doi.org/10.1016/j.neuroimage.2012.05.078.

References

Achard, S., Salvador, R., Whitcher, B., Suckling, J., Bullmore, E., 2006. A resilient, low-frequency, small-world human brain functional network with highly connected association cortical hubs. J. Neurosci. 26 (1), 63–72 (Jan.).

Alemán-Gómez, Y., Melie-García, L., Valdés-Hernandez, P., 2006. IBASPM: toolbox for automatic parcellation of brain structures (June) Proc. 12th Annual Meeting of the Organization for Human Brain Mapping. Florence, Italy.

Ashburner, J., Friston, K.J., 2005. Unified segmentation (Jul) NeuroImage 26 (3), 839–851 (URL http://dx.doi.org/10.1016/j.neuroimage.2005.02.018).

Audoin, B., Davies, G.R., Finisku, L., Chard, D.T., Thompson, A.J., Miller, D.H., 2006. Localization of grey matter atrophy in early rrms. J. Neurol. 253 (11), 1495–1501 (URL http://dx.doi.org/10.1007/s00415-006-0264-2).

Barkhof, F., 2002. The clinico-radiological paradox in multiple sclerosis revisited. Curr. Opin. Neurol. 15 (3), 239–245 (URL http://journals.lww.com/co-neurology/Fulltext/2002/06000/ The_clinico_radiological_paradox_in_multiple.3.aspx).

Barkhof, F., Filippi, M., 2009. Multiple sclerosis: MRI—the perfect surrogate marker for multiple sclerosis? (Apr.) Nat. Rev. Neurol. 5 (4), 182–183 (URL http://dx.doi.org/10.1038/nrneurol.2009.31).

Barkhof, F., Calabresi, P.A., Miller, D.H., Reingold, S.C., 2009. Imaging outcomes for neuroprotection and repair in multiple sclerosis trials (May) Nat. Rev. Neurol. 5 (5), 256–266 (URL http://dx.doi.org/10.1038/nrneurol.2009.41).

Bendfeldt, K., Klöppel, S., Nichols, T.E., Smieskova, R., Kuster, P., Traud, S., Mueller-Lenke, N., Naegelin, Y., Kappos, L., Radue, E.-W., Borgwardt, S.J., 2012. Multivariate pattern classification of gray matter pathology in multiple sclerosis (Mar.) NeuroImage 60 (1), 400–408 (URL http://www.sciencedirect.com/science/article/pii/S1053811911014728).

Biswal, B., Yetkin, F., Haughton, V., Hyde, J., 1995. Functional connectivity in the motor cortex of resting human brain using echo-planar MRI. Magn. Reson. Med. 34 (4), 537–541.

Bö, L., Geurts, J., Mörk, S., Van Der Valk, P., 2006. Grey matter pathology in multiple sclerosis. Acta Neurol. Scand. 113 (Suppl. 183), 48–50 (URL http://www.scopus.com/inward/record.url?eid=2-s2. 0-33645533249&partnerID=40&md5=fb17b7b13f009d3cc7f889e03cda4129).

Bonavita, S., Gallo, A., Sacco, R., Corte, M.D., Bisecco, A., Docimo, R., Lavorgna, L., Corbo, D., Costanzo, A.D., Tortora, F., Cirillo, M., Esposito, F., Tedeschi, G., 2011. Distributed changes in default-mode resting-state connectivity in multiple sclerosis. Mult. Scler. J. 17 (4), 411–422. http://dx.doi.org/10.1177/1352458510394609.

Buckner, R., Andrews-Hanna, J., Schacter, D., 2008. The brain's default network: anatomy, function, and relevance to disease. Ann. N. Y. Acad. Sci. 1124, 1–38 (URL http://www.scopus.com/inward/record.url?eid=2-s2. 0-41949121294&partnerID=40).

Buckner, R.L., Sepulcre, J., Talukdar, T., Krienen, F.M., Liu, H., Hedden, T., Andrews-Hanna, J.R., Sperling, R.A., Johnson, K.A., 2009. Cortical hubs revealed by intrinsic functional connectivity: mapping, assessment of stability, and relation to alzheimer's disease. J. Neurosci. 29 (6), 1860–1873.

Budde, M.D., Xie, M., Cross, A.H., Song, S.-K., 2009. Axial diffusivity is the primary correlate of axonal injury in the experimental autoimmune encephalomyelitis spinal cord: a quantitative pixelwise analysis. J. Neurosci. 29 (9), 2805–2813 (URL http://www.jneurosci.org/content/29/9/2805.abstract).

Cader, S., Cifelli, A., Abu-Omar, Y., Palace, J., Matthews, P.M., 2006. Reduced brain functional reserve and altered functional connectivity in patients with multiple sclerosis (Feb) Brain 129 (Pt 2), 527–537 (URL http://dx.doi.org/10.1093/brain/awh670).

Chen, G., Ward, B.D., Xie, C., Li, W., Wu, Z., Jones, J.L., Franczak, M., Antuono, P., Li, S.-J., 2011. Classification of alzheimer disease, mild cognitive impairment, and normal cognitive status with large-scale network analysis based on resting state functional mr imaging (Apr) Radiology 259 (1), 213–221 (URL http://dx.doi.org/10.1148/radiol.10100734).

Ciccarelli, O., Toosy, A.T., Hickman, S.J., Parker, G.J.M., Wheeler-Kingshott, C.A.M., Miller, D.H., Thompson, A.J., 2005. Optic radiation changes after optic neuritis detected by tractography-based group mapping (Jul) Hum. Brain Mapp. 25 (3), 308–316 (URL http://dx.doi.org/10.1002/hbm.20101).

Cifelli, A., Matthews, P.M., 2002. Cerebral plasticity in multiple sclerosis: insights from fMRI (May) Mult. Scler. 8 (3), 193–199.

Cifelli, A., Arridge, M., Jezzard, P., Esiri, M.M., Palace, J., Matthews, P.M., 2002. Thalamic neurodegeneration in multiple sclerosis. Ann. Neurol. 52 (5), 650–653 (URL http://dx.doi.org/10.1002/ana.10326).

Compston, A., Coles, A., 2008. Multiple sclerosis (Oct) Lancet 372 (9648), 1502–1517 (URL http://dx.doi.org/10.1016/S0140-6736(08)61620-7).

Cover, K.S., Vrenken, H., Geurts, Jeroen, J.G., van Oosten, B.W., Jelles, B., Polman, C.H., Stam, C.J., van Dijk, B.W., 2006. Multiple sclerosis patients show a highly significant decrease in alpha band interhemispheric synchronization measured using MEG. Neuroimage 29 (3), 783–788. http://dx.doi.org/10.1016/j.neuroimage.2005.08.048 (Feb).

Craddock, R.C., Holtzheimer, P.E., Hu, X.P., Mayberg, H.S., 2009. Disease state prediction from resting state functional connectivity (Dec) Magn. Reson. Med. 62 (6), 1619–1628 (URL http://dx.doi.org/10.1002/mrm.22159).

Dineen, R.A., Vilisaar, J., Hlinka, J., Bradshaw, C.M., Morgan, P.S., Constantinescu, C.S., Auer, D.P., 2009. Disconnection as a mechanism for cognitive dysfunction in multiple sclerosis (Jan) Brain 132 (Pt 1), 239–249 (URL http://dx.doi.org/10.1093/brain/awn275).

Eryilmaz, H., Ville, D.V.D., Schwartz, S., Vuilleumier, P., 2011. Impact of transient emotions on functional connectivity during subsequent resting state: a wavelet correlation approach (Feb) NeuroImage 54 (3), 2481–2491 (URL http://dx.doi.org/10.1016/j.neuroimage.2010.10.021).

Ethofer, T., Van De Ville, D., Scherer, K., Vuilleumier, P., 2009. Decoding of emotional information in voice-sensitive cortices (June 23) Curr. Biol. 19 (12), 1028–1033.

Evangelou, N., Esiri, M.M., Smith, S., Palace, J., Matthews, P.M., 2000. Quantitative pathological evidence for axonal loss in normal appearing white matter in multiple sclerosis. Ann. Neurol. 47 (3), 391–395 (cited By (since 1996) 238. URL http://www.scopus.com/inward/record.url?eid=2-s2. 0-0034104079&partnerID=40&md5=0d5927019c4440e8e7abb1c2cad80da8).

Filippi, M., Agosta, F., 2010. Imaging biomarkers in multiple sclerosis (Apr) J. Magn. Reson. Imaging 31 (4), 770–788 (URL http://dx.doi.org/10.1002/jmri.22102).

Fox, M.D., Greicius, M., 2010. Clinical applications of resting state functional connectivity. Front. Syst. Neurosci. 4, 19 (URL http://dx.doi.org/10.3389/fnsys.2010.00019).

Fox, M.D., Raichle, M.E., 2007. Spontaneous fluctuations in brain activity observed with functional magnetic resonance imaging (Sep.) Nat. Rev. Neurosci. 8 (9), 700–711 (URL http://dx.doi.org/10.1038/nrn2201).

Friston, K., Williams, S., Howard, R., Frackowiak, R., Turner, R., 1996. Movement-related effects in fMRI time-series. Magn. Reson. Med. 35 (3), 346–355 (URL http://www.scopus.com/inward/record.url?eid=2-s2. 0-0030032333&partnerID=40&md5=957aefc7ca5b34ca21ee30ae9774cdb0).

Fu, L., Matthews, P.M., De Stefano, N., Worsley, K.J., Narayanan, S., Francis, G.S., Antel, J.P., Wolfson, C., Arnold, D.L., 1998. Imaging axonal damage of normal-appearing white matter in multiple sclerosis (Jan) Brain 121 (Pt 1), 103–113.

Gean-Marton, A., Vezina, L., Marton, K., Stimac, G., Peyster, R., Taveras, J., Davis, K., 1991. Abnormal corpus callosum: a sensitive and specific indicator of multiple sclerosis. Radiology 180 (1), 215–221 (URL http://www.scopus.com/inward/record.url?eid=2-s2. 0-0025878670&partnerID=40&md5=6b8eeff2ea08a4641b244e5f0461710e).

Golanov, E.V., Reis, D.J., 1996. Contribution of oxygen-sensitive neurons of the rostral ventrolateral medulla to hypoxic cerebral vasodilatation in the rat (Aug) J. Physiol. 495 (Pt 1), 201–216.

Greicius, M.D., Krasnow, B., Reiss, A.L., Menon, V., 2003. Functional connectivity in the resting brain: a network analysis of the default mode hypothesis (Jan.) Proc. Natl. Acad. Sci. U. S. A. 100 (1), 253–258 (URL http://www.pnas.org/content/100/1/253.abstract).

Greicius, M.D., Srivastava, G., Reiss, A.L., Menon, V., 2004. Defaultmode network activity distinguishes alzheimer's disease from healthy aging: evidence from functional MRI (Mar) Proc. Natl. Acad. Sci. U. S. A. 101 (13), 4637–4642 (URL http://dx.doi.org/10.1073/pnas.0308627101).

Greicius, M.D., Flores, B.H., Menon, V., Glover, G.H., Solvason, H.B., Kenna, H., Reiss, A.L., Schatzberg, A.F., 2007. Resting-state functional connectivity in major depression: abnormally increased contributions from subgenual cingulate cortex and thalamus (Sep) Biol. Psychiatry 62 (5), 429–437 (URL http://dx.doi.org/10.1016/j.biopsych.2006.09.020).

Greicius, M.D., Supekar, K., Menon, V., Dougherty, R.F., 2009. Restingstate functional connectivity reflects structural connectivity in the default mode network (Jan) Cereb. Cortex 19 (1), 72–78 (URL http://dx.doi.org/10.1093/cercor/bhn059).

Haber, S.N., Knutson, B., 2010. The reward circuit: linking primate anatomy and human imaging (Jan) Neuropsychopharmacology 35 (1), 4–26 (URL http://dx.doi.org/10.1038/npp.2009.129).

Hawellek, D.J., Hipp, J.F., Lewis, C.M., Corbetta, M., Engel, A.K., 2011. Increased functional connectivity indicates the severity of cognitive impairment in multiple sclerosis. Proc. Natl. Acad.Sci. U. S. A. 108 (47), 19066–19071.

Helekar, S.A., Shin, J.C., Mattson, B.J., Bartley, K., Stosic, M., Saldana-King, T., Montague, P.R., Hutton, G.J., 2010. Functional brain network changes associated with maintenance of cognitive function in multiple sclerosis. Front. Hum. Neurosci. 4, 219 (URL http://dx.doi.org/10.3389/fnhum.2010.00219).

Jacobs, L.D., Beck, R.W., Simon, J.H., Kinkel, R.P., Brownscheidle, C.M., Murray, T.J., Simonian, N.A., Slasor, P.J., Sandrock, A.W., 2000. Intramuscular interferon beta-1a therapy initiated during a first demyelinating event in multiple sclerosis (Sep) N. Engl. J. Med. 343 (13), 898–904 (URL http://dx.doi.org/10.1056/NEJM200009283431301).

Jafri, M.J., Pearlson, G.D., Stevens, M., Calhoun, V.D., 2008. A method for functional network connectivity among spatially independent resting state components in schizophrenia (Feb) NeuroImage 39 (4), 1666–1681 (URL http://dx.doi.org/10.1016/j.neuroimage.2007.11.001).

Jones, D.T., Mateen, F.J., Lucchinetti, C.F., Jack Jr., C.R., Welker, K.M., 2011. Default mode network disruption secondary to a lesion in the anterior thalamus (Feb) Arch. Neurol. 68 (2), 242–247 (URL http://dx.doi.org/10.1001/archneurol.2010.259).

Kamitani, Y., Tong, F., 2005. Decoding the visual and subjective contents of the human brain. Nat. Neurosci. 8, 679–685.

Kappos, L., Freedman, M.S., Polman, C.H., Edan, G., Hartung, H.-P., Miller, D.H., Montalbán, X., Barkhof, F., Radü, E.-W., Bauer, L., Dahms, S., Lanius, V., Pohl, C., Sandbrink, R., B. E. N. E. F. I. T. Study Group, 2007. Effect of early versus delayed interferon beta-1b treatment on disability after a first clinical event suggestive of multiple sclerosis: a 3-year follow-up analysis of the BENEFIT study (Aug) Lancet 370 (9585), 389–397.

Kensinger, E.A., Schacter, D.L., 2008. Neural processes supporting young and older adults' emotional memories. J. Cogn. Neurosci. 20 (7), 1161–1173 (URL http://www.mitpressjournals.org/doi/abs/10.1162/jocn.2008. 20080).

Kurtzke, J.F., 1983. Rating neurologic impairment in multiple sclerosis: an expanded disability status scale (EDSS) (Nov) Neurology 33 (11), 1444–1452.

Langs, G., Menze, B.H., Lashkari, D., Golland, P., 2011. Detecting stable distributed patterns of brain activation using gini contrast. NeuroImage 56 (2), 497–507

(URL http://www.sciencedirect.com/science/article/B6WNP-50S8PM9-1/2/40411edede5ff716c2502fe4bff8dc05).
Lee, M., Reddy, H., Johansen-Berg, H., Pendlebury, S., Jenkinson, M., Smith, S., Palace, J., Matthews, P.M., 2000. The motor cortex shows adaptive functional changes to brain injury from multiple sclerosis (May) Ann. Neurol. 47 (5), 606–613.
Li, S.-J., Li, Z., Wu, G., Zhang, M.-J., Franczak, M., Antuono, P.G., 2002. Alzheimer disease: evaluation of a functional MR imaging index as a marker (Oct) Radiology 225 (1), 253–259.
Lin, X., Tench, C.R., Morgan, P.S., Niepel, G., Constantinescu, C.S., 2005. importance sampling' in ms: use of diffusion tensor tractography to quantify pathology related to specific impairment (Oct) J. Neurol. Sci. 237 (1-2), 13–19 (URL http://dx.doi.org/10.1016/j.jns.2005.04.019).
Liu, Y., Liang, P., Duan, Y., Jia, X., Yu, C., Zhang, M., Wang, F., Zhang, M., Dong, H., Ye, J., Butzkueven, H., Li, K., 2011. Brain plasticity in relapsing-remitting multiple sclerosis: evidence from resting state fMRI (Feb) J. Neurol. Sci. 304 (1-2), 127–131 (URL http://dx.doi.org/10.1016/j.jns.2011.01.023).
Logothetis, N.K., 2008. What we can do and what we cannot do with fMRI (Jun) Nature 453 (7197), 869–878 (URL http://dx.doi.org/10.1038/nature06976).
Lowe, M.J., Mock, B.J., Sorenson, J.A., 1998. Functional connectivity in single and multislice echoplanar imaging using resting state fluctuations (Feb.) NeuroImage 7 (2), 119–132 (URL http://www.sciencedirect.com/science/article/B6WNP-45M2Y15-1G/2/88964e40762eb2eadd8376e575d6e198).
Lowe, M.J., Beall, E.B., Sakaie, K.E., Koenig, K.A., Stone, L., Marrie, R.A., Phillips, M.D., 2008. Resting state sensorimotor functional connectivity in multiple sclerosis inversely correlates with transcallosal motor pathway transverse diffusivity (Jul) Hum. Brain Mapp. 29 (7), 818–827 (URL http://dx.doi.org/10.1002/hbm.20576).
Mainero, C., Caramia, F., Pozzilli, C., Pisani, A., Pestalozza, I., Borriello, G., Bozzao, L., Pantano, P., 2004. fMRI evidence of brain reorganization during attention and memory tasks in multiple sclerosis (Mar) NeuroImage 21 (3), 858–867 (URL http://dx.doi.org/10.1016/j.neuroimage.2003.10.004).
Manson, S.C., Palace, J., Frank, J.A., Matthews, P.M., 2006. Loss of interhemispheric inhibition in patients with multiple sclerosis is related to corpus callosum atrophy (Oct) Exp. Brain Res. 174 (4), 728–733 (URL http://dx.doi.org/10.1007/s00221-006-0517-4).
Manson, S.C., Wegner, C., Filippi, M., Barkhof, F., Beckmann, C., Ciccarelli, O., Stefano, N.D., Enzinger, C., Fazekas, F., Agosta, F., Gass, A., Hirsch, J., Johansen-Berg, H., Kappos, L., Korteweg, T., Polman, C., Mancini, L., Manfredonia, F., Marino, S., Miller, D.H., Montalban, X., Palace, J., Rocca, M., Ropele, S., Rovira, A., Smith, S., Thompson, A., Thornton, J., Yousry, T., Frank, J.A., Matthews, P.M., 2008. Impairment of movementassociated brain deactivation in multiple sclerosis: further evidence for a functional pathology of interhemispheric neuronal inhibition (May) Exp. Brain Res. 187 (1), 25–31 (URL http://dx.doi.org/10.1007/s00221-008-1276-1).
Mantini, D., Perrucci, M.G., Gratta, C.D., Romani, G.L., Corbetta, M., 2007. Electrophysiological signatures of resting state networks in the human brain (Aug) Proc. Natl. Acad. Sci. U. S. A. 104 (32), 13170–13175 (URL http://dx.doi.org/10.1073/pnas.0700668104).
Mesaros, S., Rocca, M.A., Riccitelli, G., Pagani, E., Rovaris, M., Caputo, D., Ghezzi, A., Capra, R., Bertolotto, A., Comi, G., Filippi, M., 2009. Corpus callosum damage and cognitive dysfunction in benign MS (Aug) Hum. Brain Mapp. 30 (8), 2656–2666 (URL http://dx.doi.org/10.1002/hbm.20692).
Miller, D.H., Thompson, A.J., Filippi, M., 2003. Magnetic resonance studies of abnormalities in the normal appearing white matter and greymatter in multiple sclerosis (Dec) J. Neurol. 250 (12), 1407–1419 (URL http://dx.doi.org/10.1007/s00415-003-0243-9).
Minden, S.L., Schiffer, R.B., 1990. Affective disorders in multiple sclerosis. review and recommendations for clinical research (Jan) Arch. Neurol. 47 (1), 98–104.
Morgen, K., Kadom, N., Sawaki, L., Tessitore, A., Ohayon, J., McFarland, H., Frank, J., Martin, R., Cohen, L.G., 2004. Training-dependent plasticity in patients with multiple sclerosis (Nov) Brain 127 (Pt 11).
Morgen, K., Sammer, G., Courtney, S.M., Wolters, T., Melchior, H., Blecker, C.R., Oschmann, P., Kaps, M., Vaitl, D., 2007. Distinct mechanisms of altered brain activation in patients with multiple sclerosis (Sep) NeuroImage 37 (3), 937–946 (URL http://dx.doi.org/10.1016/j.neuroimage.2007.05.045).
Mourao-Miranda, J., Bokde, A.L., Born, C., Hampel, H., Stetter, M., 2005. Classifying brain states and determining the discriminating activation patterns: support vector machine on functional MRI data (Dec.) NeuroImage 28 (4), 980–995 (URL http://www.sciencedirect.com/science/article/B6WNP-4HGM79R-1/2/fcb89095569ad4445086c71d6eb5bfff).
Muehlhan, M., Lueken, U., Wittchen, H.-U., Kirschbaum, C., 2011. The scanner as a stressor: evidence from subjective and neuroendocrine stress parameters in the time course of a functional magnetic resonance imaging session (Feb) Int. J. Psychophysiol. 79 (2), 118–126 (URL http://dx.doi.org/10.1016/j.ijpsycho.2010.09.009).
Noseworthy, J.H., Lucchinetti, C., Rodriguez, M., Weinshenker, B.G., 2000. Multiple sclerosis (Sep.) N. Engl. J. Med. 343 (13), 938–952 (URL http://content.nejm.org).
Olson, I.R., Plotzker, A., Ezzyat, Y., 2007. The enigmatic temporal pole: a review of findings on social and emotional processing (Jul) Brain 130 (Pt 7), 1718–1731 (URL http://dx.doi.org/10.1093/brain/awm052).
Pelletier, J., Suchet, L., Witjas, T., Habib, M., Guttmann, C.R., Salamon, G., Lyon-Caen, O., Chérif, A.A., 2001. A longitudinal study of callosal atrophy and interhemispheric dysfunction in relapsing-remitting multiple sclerosis Jan Arch. Neurol. 58 (1), 105–111.
Polman, C.H., Reingold, S.C., Edan, G., Filippi, M., Hartung, H.-P., Kappos, L., Lublin, F.D., Metz, L.M., McFarland, H.F., O'Connor, P.W., Sandberg-Wollheim, M., Thompson, A.J., Weinshenker, B.G., Wolinsky, J.S., 2005. Diagnostic criteria for multiple sclerosis: 2005 revisions to the McDonald criteria. Ann. Neurol. 58 (6), 840–846 (URL http://dx.doi.org/10.1002/ana.20703).
Polman, C.H., Reingold, S.C., Banwell, B., Clanet, M., Cohen, J.A., Filippi, M., Fujihara, K., Havrdova, E., Hutchinson, M., Kappos, L., Lublin, F.D., Montalban, X., O'Connor, P., Sandberg-Wollheim, M., Thompson, A.J., Waubant, E., Weinshenker, B., Wolinsky, J.S., 2011. Diagnostic criteria for multiple sclerosis: 2010 revisions to the McDonald criteria (Feb) Ann. Neurol. 69 (2), 292–302 (URL http://dx.doi.org/10.1002/ana.22366).
Prinster, A., Quarantelli, M., Orefice, G., Lanzillo, R., Brunetti, A., Mollica, C., Salvatore, E., Brescia Morra, V., Coppola, G., Vacca, G., Alfano, B., Salvatore, M., 2006. Grey matter loss in relapsing–remitting multiple sclerosis: a voxel-based morphometry study. NeuroImage 29, 859–867.
Raichle, M.E., MacLeod, A.M., Snyder, A.Z., Powers, W.J., Gusnard, D.A., Shulman, G.L., 2001. A default mode of brain function (Jan) Proc. Natl. Acad. Sci. U. S. A. 98 (2), 676–682 (URL http://dx.doi.org/10.1073/pnas.98.2.676).
Rashid, W., Parkes, L., Ingle, G., Chard, D., Toosy, A., Altmann, D., Symms, M., Tofts, P., Thompson, A., Miller, D., 2004. Abnormalities of cerebral perfusion in multiple sclerosis. J. Neurol. Neurosurg. Psychiatry 75 (9), 1288–1293 (URL http://www.scopus.com/inward/record.url?eid=2-s2.0-4344661629&partnerID=40&md5=f852ccf9dc516189d966445fd6cce419).
Ratchford, J.N., Calabresi, P.A., 2008. The diagnosis of MS: white spots and red flags. Neurology 70 (13 Part 2), 1071–1072 (URL http://www.neurology.org).
Reddy, H., Narayanan, S., Matthews, P.M., Hoge, R.D., Pike, G.B., Duquette, P., Antel, J., Arnold, D.L., 2000a. Relating axonal injury to functional recovery in ms (Jan) Neurology 54 (1), 236–239.
Reddy, H., Narayanan, S., Arnoutelis, R., Jenkinson, M., Antel, J., Matthews, P.M., Arnold, D.L., 2000b. Evidence for adaptive functional changes in the cerebral cortex with axonal injury from multiple sclerosis Nov Brain 123 (Pt11), 2314–2320.
Reich, D.S., Smith, S.A., Gordon-Lipkin, E.M., Ozturk, A., Caffo, B.S., Balcer, L.J., Calabresi, P.A., 2009. Damage to the optic radiation in multiple sclerosis is associated with retinal injury and visual disability (Aug) Arch. Neurol. 66 (8), 998–1006 (URL http://dx.doi.org/10.1001/archneurol.2009 107).
Richiardi, J., Van De Ville, D., Riesen, K., Bunke, H., 2010. Vector space embedding of undirected graphs with fixed-cardinality vertex sequences for classification. Proc. 20th Int. Conf. on Pattern Recognition (ICPR), pp. 902–905.
Richiardi, J., Eryilmaz, H., Schwartz, S., Vuilleumier, P., Van De Ville, D., 2011. Decoding brain states from fMRI connectivity graphs (May) NeuroImage 56 (2), 616–626 (Special Issue on Multivariate Decoding and Brain Reading).
Rocca, M.A., Filippi, M., 2007. Functional MRI in multiple sclerosis (Apr) J. Neuroimaging 17 (Suppl. 1), 36S–41S (URL http://dx.doi.org/10.1111/j.1552-6569.2007.00135.x).
Rocca, M.A., Pagani, E., Absinta, M., Valsasina, P., Falini, A., Scotti, G., Comi, G., Filippi, M., 2007. Altered functional and structural connectivities in patients with MS: a 3-T study (Dec) Neurology 69 (23), 2136–2145 (URL http://dx.doi.org/10.1212/01.wnl.0000295504.92020.ca).
Rocca, M.A., Valsasina, P., Absinta, M., Riccitelli, G., Rodegher, M.E., Misci, P., Rossi, P., Falini, A., Comi, G., Filippi, M., 2010. Default-mode network dysfunction and cognitive impairment in progressive MS (Apr) Neurology 74 (16), 1252–1259 (URL http://dx.doi.org/10.1212/WNL.0b013e3181d9ed91).
Rolak, L.A., Fleming, J.O., 2007. The differential diagnosis of multiple sclerosis (March) Neurologist 13 (2), 57–72.
Roosendaal, S.D., Schoonheim, M.M., Hulst, H.E., Sanz-Arigita, E.J., Smith, S.M., Geurts, J.J.G., Barkhof, F., 2010. Resting state networks change in clinically isolated syndrome (Jun) Brain 133 (Pt 6), 1612–1621 (URL http://dx.doi.org/10.1093/brain/awq058).
Rousseeuw, P.J., Driessen, K.V., 1998. A fast algorithm for the minimum covariance determinant estimator. Technometrics 41, 212–223.
Rovira, A., Swanton, J., Tintore, M., Huerga, E., Barkhof, F., Filippi, M., Frederiksen, J.L., Langkilde, A., Miszkiel, K., Polman, C., Rovaris, M., Sastre-Garriga, J., Miller, D., Montalban, X., 2009. A single, early magnetic resonance imaging study in the diagnosis of multiple sclerosis (May) Arch. Neurol. 66 (5), 587–592 (URL http://archneur.ama-assn.org/cgi/content/abstract/66/5/587).
Salvador, R., Suckling, J., Coleman, M.R., Pickard, J.D., Menon, D., Bullmore, E., 2005. Neurophysiological architecture of functional magnetic resonance images of human brain (Sep) Cereb. Cortex 15 (9), 1332–1342 (URL http://dx.doi.org/10.1093/cercor/bhi016).
Shirer, W.R., Ryali, S., Rykhlevskaia, E., Menon, V., Greicius, M.D., 2011. Decoding subject-driven cognitive states with whole-brain connectivity patterns. Cereb. Cortex. http://dx.doi.org/10.1093/cercor/bhr099.
Song, S.-K., Sun, S.-W., Ju, W.-K., Lin, S.-J., Cross, A.H., Neufeld, A.H., 2003. Diffusion tensor imaging detects and differentiates axon and myelin degeneration in mouse optic nerve after retinal ischemia (Nov) NeuroImage 20 (3), 1714–1722.
Swanton, J.K., Rovira, A., Tintore, M., Altmann, D.R., Barkhof, F., Filippi, M., Huerga, E., Miszkiel, K.A., Plant, G.T., Polman, C., Rovaris, M., Thompson, A.J., Montalban, X., Miller, D.H., 2007. Mri criteria for multiple sclerosis in patients presenting with clinically isolated syndromes: a multicentre retrospective study (August) Lancet Neurol. 6 (8), 677–686 (URL http://dx.doi.org/10.1016/S1474-4422(07)70176-X).
Trapp, B.D., Peterson, J., Ransohoff, R.M., Rudick, R., Mork, S., Bo, L., 1998. Axonal transection in the lesions of multiple sclerosis (Jan.) N. Engl. J. Med. 338 (5), 278–285 (URL http://content.nejm.org/cgi/content/abstract/338/5/278).
Tzourio-Mazoyer, N., Landeau, B., Papathanassiou, D., Crivello, F., Etard, O., Delcroix, N., Mazoyer, B., Joliot, M., 2002. Automated anatomical labeling of activations in SPM using a macroscopic anatomical parcellation of the MNI MRI single-subject brain. NeuroImage 15, 273–289.
Vercellino, M., Masera, S., Lorenzatti, M., Condello, C., Merola, A., Mattioda, A., Tribolo, A., Capello, E., Mancardi, G.L., Mutani, R., Giordana, M.T., Cavalla, P., 2009. Demyelination, inflammation, and neurodegeneration in multiple sclerosis deep gray

matter (May) J. Neuropathol. Exp. Neurol. 68 (5), 489–502 (URL http://dx.doi.org/10.1097/NEN.0b013e3181a19a5a).
Weil, R.S., Rees, G., 2010. Decoding the neural correlates of consciousness (Dec) Curr. Opin. Neurol. 23 (6), 649–655 (URL http://dx.doi.org/10.1097/WCO.0b013e32834028c7).
Weygandt, M., Hackmack, K., Pfüller, C., Bellmann–Strobl, J., Paul, F., Zipp, F., Haynes, J., 2011. Mri pattern recognition in multiple sclerosis normalappearing brain areas (Jun.) PLoS One 6 (6), e21138–e (URL http://dx.doi.org/10.1371%2Fjournal.pone.0021138).
Wylezinska, M., Cifelli, A., Jezzard, P., Palace, J., Alecci, M., Matthews, P.M., 2003. Thalamic neurodegeneration in relapsing-remitting multiple sclerosis. Neurology 60 (12), 1949–1954 (URL http://www.neurology.org/content/60/12/1949.abstract).
Yaldizli, O., Glassl, S., Sturm, D., Papadopoulou, A., Gass, A., Tettenborn, B., Putzki, N., 2011. Fatigue and progression of corpus callosum atrophy in multiple sclerosis. J. Neurol. 258 (12), 2199–2205. http://dx.doi.org/10.1007/s00415-011-6091-0 (Dec).
Zhu, B., Moore, G.R., Zwimpfer, T.J., Kastrukoff, L.F., Dyer, J.K., Steeves, J.D., Paty, D.W., Cynader, M.S., 1999. Axonal cytoskeleton changes in experimental optic neuritis (Apr) Brain Res. 824 (2), 204–217.